PHYSICAL REVIEW D **81,** 043524 (2010)

Tachyonic resonance preheating in an expanding universe

Ali Akbar Abolhasani,[1,2,*] Hassan Firouzjahi,[2,†] and M. M. Sheikh-Jabbari[2,‡]

[1]*Department of Physics, Sharif University of Technology, Tehran, Iran*

[2]*School of Physics, Institute for Research in Fundamental Sciences (IPM), P.O. Box 19395-5531, Tehran, Iran*

(Received 11 December 2009; published 12 February 2010)

In this paper the tachyonic resonance preheating generated from the bosonic trilinear $\phi\chi^2$ interactions in an expanding universe is studied. In $\lambda\phi^4/4$ inflationary model the trilinear interaction, in contrast to the four-legs $\phi^2\chi^2$, breaks the conformal symmetry explicitly and the resonant source term becomes nonperiodic, making the Floquet theorem inapplicable. We find that the occupation number of the produced χ particles has a nonlinear exponential growth with exponent $\sim x^{3/2}$, where x is the conformal time. This should be contrasted with preheating from a periodic resonant source arising, for example, from the four-legs $\phi^2\chi^2$ interaction, where the occupation number has a linear exponential growth. We present an analytic method to compute the interference term coming from phases accumulated in nontachyonic scattering regions and show that the effects of the interference term cause ripples on $x^{3/2}$ curve, a result which is confirmed by numerical analysis. Studying the effects of backreaction of the χ particles, we show that tachyonic resonance preheating in our model can last long enough to transfer most of the energy from the background inflation field ϕ, providing an efficient model for preheating in the chaotic inflation models.

DOI: 10.1103/PhysRevD.81.043524 PACS numbers: 98.80.Cq

I. INTRODUCTION

At the end of inflation the Universe is extremely cold and all of its energy is concentrated in the inflaton field ϕ. Therefore, the reheating stage is a key ingredient to connect a successful inflationary stage into hot big bang cosmology. In simplest models of inflation, such as chaotic inflation models, the inflaton field oscillates coherently around the minimum of the potential with amplitude close to the Planck mass, M_P.[1] To transfer the energy from the background inflaton field and reheat the Universe one has to consider its coupling to other fields, such as the standard model fields. Because of coherent oscillations of the background inflaton field around the potential minimum, explosive particle creation can happen via parametric resonance which can drag most of the energy from the inflaton field and reheat the Universe [1–4]. Preheating, the stage of explosive particle creation via parametric resonance, is a nonperturbative effect and the produced particles are highly nonthermal. Subsequent turbulent interactions of different modes and rescatterings would bring an end to preheating and thermalization starts [5–10] where the perturbative reheating mechanism may start [11,12]. For a review of preheating, see [13] and references therein.

There have been many studies of preheating via four-legs interaction $g^2\phi^2\chi^2$ between the inflaton field and the resonance field χ in expanding or flat backgrounds. One disadvantage of $g^2\phi^2\chi^2$ preheating channel is that the decay of inflaton in an expanding background is not complete and the inhomogeneous inflaton particles will dominate with the matter equation of state, an unsatisfactory state to end (p)reheating with.

In order to enhance the preheating mechanism other interactions are necessary, specially once the inflaton field amplitude is damped while oscillating around its minimum. The simplest and the most natural of these interactions is the trilinear interaction $\sigma\phi\chi^2$ where σ is a constant of dimension of mass. The implications of trilinear interaction for the chaotic inflationary potential $m^2\phi^2/2$ was studied in [14]. One interesting aspect of preheating via trilinear interaction is that during half period of its oscillation, the inflaton field has the opposite sign and the time-dependent frequency squared for the χ particle creation becomes negative for small enough mode wavelengths. This tachyonic instability enhances the preheating mechanism significantly and in [14] was dubbed as ''tachyonic resonance.'' The analysis of [14] was mainly devoted to a flat background and the effects of tachyonic resonance in an expanding background was briefly considered, incorporating them ''adiabatically.'' The tachyonic effect of a trilinear interaction was used in [15], in the context of cosmological moduli problem and the idea of tachyonic parametric resonance with a negative coupling constant was also exploited in [16].

Here we consider the tachyonic resonance preheating in $\lambda\phi^4/4$ and $m^2\phi^2/2$ inflationary potentials in an expanding universe. Our main interest will be in the $\lambda\phi^4/4$ theory but we extend the results of [14] for $m^2\phi^2/2$ inflationary model to an expanding background.

*abolhasani@ipm.ir
†firouz@ipm.ir
‡jabbari@theory.ipm.ac.ir

[1]We use the convention in which $M_P^2 = 1/G_N$, for G_N being the Newton constant.

The preheating with four-leg interaction within the $\lambda\phi^4/4$ inflation theory was studied extensively in [17,18]. Because of the conformal invariance of the inflationary potential, the effects of an expanding background can be absorbed by a conformal transformation and one is basically dealing with preheating in a Minkowski background. However, with the addition of $\sigma\phi\chi^2$ interaction, the conformal invariance is broken explicitly and the methods employed in [17] should now be modified. Breaking of conformal invariance results in an explicit breaking of periodicity in the χ-modes equation: the amplitude of the source term in χ-field particle creation grows linearly with the dimensionless conformal time x. Consequently, the standard Floquet theorem does not apply. This leads to the interesting result that the number density of χ particles produced at momentum $\mathbf{k}$, $n_{\mathbf{k}}$, grows as $e^{cx^{3/2}}$ for some constant c. This should be compared with the standard result of the preheating due to a periodic source term, where $n_{\mathbf{k}}$ has a linear exponential growth as dictated by the Floquet theorem.

Another interesting result of our analysis is that we present an analytic method to compute the interference term which accounts for the phase difference between the χ fields during each period of the ϕ field oscillation. The phase accumulated during certain number of oscillations, which we compute, makes the χ particle creation to be destructive for certain modes, the k^2 which we specify. This causes some ripples on the $x^{3/2}$ curve in the $\ln n_{\mathbf{k}}$ diagram. This result is to be compared with the stochastic nature of the phases in the four-leg preheating scenarios [1,17].

While our main interest is in $\lambda\phi^4/4$ inflationary theory, we also study the effect of expanding background on $m^2\phi^2/2$ theory. As one may expect, the effect of expanding background will generally suppress the preheating efficiency. As we demonstrate, however, it actually enhances the preheating for some certain modes.

As the number of χ particles grows their backreaction on the dynamics of the particle production and the ϕ field dynamics becomes important, slowing down the preheating and eventually terminating it. For a successful preheating model it is necessary that this backreaction does not become large too early, before the energy of the inflaton field is completely transferred into the ϕ or χ particles. It is also important that in the end of preheating we remain with a relativistic ensemble of these particles. As in the case of $m^2\phi^2$, which has been analyzed in [14], our analysis shows that the trilinear interactions seem to lead to a more efficient preheating than the four-leg case.

The paper is organized as follows. In Sec. II we study in detail the tachyonic resonance for $\lambda\phi^4/4$ theory. We demonstrate that our analytical results agree very well with the exact numerical results. In Sec. III we repeat the analysis of tachyonic resonance for $m^2\phi^2/2$ theory in an expanding background. In Sec. IV we study the effects of χ-particle backreactions on the preheating and estimate the time preheating ends. A summary of the results is given in Sec. V. Some technical aspects of the analysis are relegated to Appendixes A, B, C, and D.

II. THE TACHYONIC RESONANCE IN $\lambda\phi^4/4$ THEORY

As explained above, we are mainly interested in tachyonic resonance in $\lambda\phi^4/4$ inflationary theory with the trilinear interaction $\sigma\phi\chi^2$, where σ is a parameter with dimension of mass. As in [14] we have to include the self-interaction $\lambda'\chi^4$ to uplift the potential and keep it bounded from below. The total potential is

$$V = \frac{\lambda}{4}\phi^4 + \frac{\sigma}{2}\phi\chi^2 + \frac{\lambda'}{4}\chi^4 + \frac{\sigma^4}{16\lambda\lambda'^2} \tag{1}$$

$$= \lambda\left(\frac{\phi^2}{2} - \frac{\sigma^2}{4\lambda\lambda'}\right)^2 + \frac{\lambda'}{4}\left(\chi^2 + \frac{\sigma\phi}{\lambda'}\right)^2. \tag{2}$$

The potential has a global minimum at $\phi_0 = -\sqrt{\sigma^2/2\lambda\lambda'}$ and $\chi_0^2 = -\sigma\phi_0/\lambda'$. The last term in (1) is added to lift the global minimum to zero. In order to make sure that this constant value does not contribute to the inflationary dynamics, we require that $\sigma^4/\lambda\lambda'^2 \ll \lambda\phi_{\rm end}^4$, where $\phi_{\rm end}$ is the value of the inflaton field at the end of inflation when the onset of preheating starts with $\phi_{\rm end} \simeq M_P/\sqrt{\pi}$. This leads to

$$\frac{\sigma}{\sqrt{\lambda\lambda'}M_P} \ll 1. \tag{3}$$

If we assume that the χ field is heavy during inflation and is settled down to its minimum at χ_0 this requires that $12\sigma M_P^2/\lambda\phi^3 > 1$, which can be satisfied if $12\sigma M_P^2/\lambda\phi_i^3 > 1$, where ϕ_i is the initial value of the inflaton field at the start of inflation. For inflation to solve the flatness and the horizon problem, we require that $\phi_i \simeq 10M_P$ and $\lambda \simeq 10^{-14}$. So the assumption that the field χ would be stabilized in its minimum requires that

$$\frac{\sigma}{\lambda M_P} \gtrsim 10^2. \tag{4}$$

However, it is also possible that the field χ is light during inflation and can then contribute to isocurvature perturbations.

To study the preheating with trilinear interaction, we review the background of [17] where the parametric resonance with four-legs interaction for $\lambda\phi^4/4$ theory was investigated. As in [17], performing the conformal transformation $\varphi \equiv a(\eta)\phi$ the background equation for the φ field to a very good approximation is simplified to

$$\varphi'' + \lambda\varphi^3 = 0, \tag{5}$$

where the derivatives are with respect to the conformal time $d\eta = dt/a(t)$, where $a(t)$ is the scale factor. Here we

neglected a'' in Eq. (5) because the scale factor evolves to a very good approximation as in a radiation dominated era. The solution to this equation is given in terms of Jacobi elliptic cosine function

$$\varphi = \tilde{\varphi} f(x), \tag{6}$$

where $\tilde{\varphi}$ is the amplitude of the oscillations at the onset of preheating which we take to be $0.1M_P$, and the dimensionless conformal time x is defined by

$$x \equiv \sqrt{\lambda}\tilde{\varphi}\,\eta = \left(\frac{6\lambda M_P^2}{\pi}\right)^{1/4}\sqrt{t}. \tag{7}$$

The Jacobi elliptic cosine function satisfies the relation $f'^2 = \frac{1}{2}(1 - f^4)$ with the solution denoted by[2]

$$f(x) = cn\left(x, \frac{1}{2}\right). \tag{8}$$

The function $f(x)$ is a periodic function with the periodicity

$$T \equiv 4K(1/2) \simeq 7.416, \tag{9}$$

where $K(m)$ represents the complete elliptic integral of the first kind. For a review of Jacobi elliptic cosine function, see Appendix A.

One also notes that the following relations also hold:

$$a(\eta) = \sqrt{\frac{2\pi\lambda}{3}}\frac{\tilde{\varphi}^2}{M_p}\eta = \sqrt{\frac{2\pi}{3}}\frac{\tilde{\varphi}}{M_p}x, \qquad t = \sqrt{\frac{\pi\lambda}{6}}\frac{\tilde{\varphi}^2}{M_p}\eta^2. \tag{10}$$

Ignoring the backreaction of the produced χ particles, performing the conformal transformation $\hat{\chi} = a(\eta)\chi$, and using the background Eqs. (10), the equation for the mode function $\chi_{\mathbf{k}}$ in momentum space is

$$\hat{\chi}''_{\mathbf{k}} + (\kappa^2 + pxf(x))\hat{\chi}_{\mathbf{k}} = 0, \tag{11}$$

where the derivatives are now with respect to the dimensionless conformal time x given in (7), and

$$\kappa^2 = \frac{\mathbf{k}^2}{\lambda\tilde{\varphi}^2}, \qquad p \equiv \sqrt{\frac{2\pi}{3}}\left(\frac{\sigma}{\lambda M_p}\right). \tag{12}$$

In writing (11) we have ignored the χ_0 and ϕ_0 terms, associated with the minima of the potential (1). The effects of nonzero values for χ_0 and ϕ_0 will appear in (11) as the shift in p by an amount of the order $p\frac{\phi_0}{\tilde{\varphi}}$ (and similarly for the κ^2 term). This causes an error of the order $p\sqrt{\frac{\lambda}{\lambda'}}$, which is much smaller than 1 as can be seen from Eq. (3).

Before we start the analytical theory of tachyonic resonance, we need to estimate the magnitude of parameter p. This in turn is determined by the conditions whether the field χ is heavy or light during inflation. If we assume that the field χ is heavy during inflation, then the condition (4) indicates that $p \geq 100$. However, if we assume that the field χ is light during inflation, which is our preferred choice, then (3) can be used to estimate the bound on p. Writing (3) in the form $p\sqrt{\lambda/\lambda'} \ll 1$, we see that for natural choice of $\lambda \sim \lambda'$, $p \ll 1$. On the other hand, for $\lambda' \gg \lambda$, the bound on p may become relaxed. We present our analytical results for arbitrary value of p. However, for numerical examples we shall consider the cases $p \ll 1$ and $p \sim 1$ for illustrations.

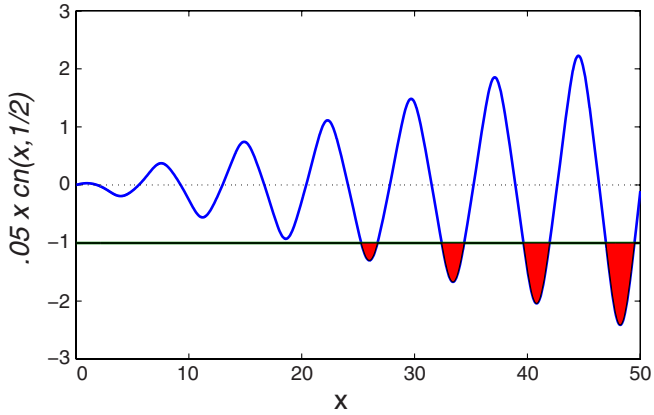

FIG. 1 (color online). A plot of $pxf(x)$ given by (13) is presented here for $p = 0.05$. The horizontal line represents the solutions of $\omega^2(x) = \kappa^2 + pxf(x) = 0$ for $\kappa^2 = 1$. The filled regions shows the tachyonic regions where $\omega^2(x) < 0$. In our notation, the jth tachyonic region is confined to $x_j^- < x < x_j^+$.

Equation (11) represents a harmonic oscillator with the time-dependent frequency

$$\omega^2(x) \equiv \kappa^2 + pxf(x) = \kappa^2 + pxcn\left(x, \frac{1}{2}\right). \tag{13}$$

A plot of $pxf(x)$ is given in Fig. 1. We see that $\omega^2(x)$ is not periodic and its maximum value is increasing linearly with the conformal time x. Consequently, the Floquet theorem for particle creation via parametric resonance with a periodic source does not apply. We need to employ the direct scattering method to evaluate the number density of the χ particle, $n_{\mathbf{k}}$. For a given $\kappa^2 \neq 0$, $\omega^2(x)$ is initially positive. However, for $t > t_\star$ it becomes tachyonic and the method of tachyonic resonance considered in [14] would apply. Interestingly, the zero-momentum case, $\kappa = 0$, is tachyonic for all the time. We therefore start our analytical study of tachyonic resonance with this simple case and defer the case of $\kappa^2 \neq 0$ to Sec. II B.

A. Tachyonic resonance with $\kappa^2 = 0$

As can be seen from Fig. 1, $\omega^2(x)$ becomes negative in the region where $f(x) < 0$. The Jacobi elliptic cosine is periodic with period $T = 4K(1/2)$ and has roots at

[2]Our definition of Jacobi elliptic cosine conforms to that of [19] which is slightly different than that of [17].

$$x_j^- = \left(j - \frac{3}{4}\right)T, \qquad x_j^+ = \left(j - \frac{1}{4}\right)T, \tag{14}$$

where the integer number $j = 1, 2, \ldots$ counts the number of oscillations of $f(x)$ starting from $x = 0$. In this convention, the jth tachyonic region is confined to $x_j^- < x < x_j^+$. Similarly, the minima and the maxima of $f(x)$ are given by

$$x_j^{\max} = (j-1)T, \qquad x_j^{\min} = \left(j - \frac{1}{2}\right)T. \tag{15}$$

In the region $x_j^- < x < x_j^+$, $\omega^2(x) < 0$ and the method of tachyonic resonance developed in [14] applies.

As in [14], in the region $\omega^2(x) > 0$ and when the adiabaticity condition $|\omega|'/\omega^2 \ll 1$ holds, the solution of (11) can be given in WKB approximation as

$$\hat{\chi}_{\mathbf{k}=0}(x) \simeq \frac{\alpha^j}{\sqrt{2\omega(x)}} \exp\left(-i\int_{x_0}^{x} \omega(x')dx'\right) + \frac{\beta^j}{\sqrt{2\omega(x)}} \exp\left(+i\int_{x_0}^{x} \omega(x')dx'\right), \tag{16}$$

where α^j and β^j are the Bogoliubov coefficients with normalization $|\alpha|^2 - |\beta|^2 = 1$. At the beginning of preheating when the inflaton field starts its oscillation toward the potential minimum, there is no χ particle and we start with the vacuum initial condition $\alpha^0 = 1$ and $\beta^0 = 0$. The occupation number of the χ particle after j oscillation (or after j tachyonic regions) is given by

$$n^j_{\mathbf{k}=0} = |\beta^j|^2. \tag{17}$$

For the tachyonic region $x_j^- < x < x_j^+$, the WKB approximation holds again for the frequency $\Omega^2(x) \equiv -\omega^2(x)$ and the solution is given as a superposition of exponentially growing and decaying parts:

$$\hat{\chi}_{\mathbf{k}=0}(x) \simeq \frac{a^j}{\sqrt{2\Omega(x)}} \exp\left(-\int_{x_-^j}^{x} \Omega(x')dx'\right) + \frac{b^j}{\sqrt{2\Omega(x)}} \exp\left(+\int_{x_-^j}^{x} \Omega(x')dx'\right), \tag{18}$$

where a^j and b^j are constants of integration. Finally, after $x > x_+^j$, the solution is given by (16) with $j \to j + 1$.

Around the points x_-^j and x_+^j where the adiabatic approximation is broken, we have to solve the mode equation (11) as in scattering theory and match it with the solutions (16) and (18). Following the methods of [14] in performing this matching condition, we obtain the following transfer matrix, relating the Bogoliubov coefficients after $j^{\text{th}} + 1$ scattering to those of jth scattering via

$$\begin{pmatrix} \alpha^{j+1} \\ \beta^{j+1} \end{pmatrix} = e^{X^j} \begin{pmatrix} 1 & ie^{2i\theta^j} \\ -ie^{-2i\theta^j} & 1 \end{pmatrix} \begin{pmatrix} \alpha^j \\ \beta^j \end{pmatrix}, \tag{19}$$

where

$$X^j = \int_{x_-^j}^{x_+^j} \Omega(z)dz, \tag{20}$$

and θ^j is the total phase accumulated from x_0 to x_j^- during the nontachyonic intervals, where $\omega^2 > 0$. In our case, we have $\theta^j = \theta^0 + \sum_j \Theta^j$, where θ^0 is an initial phase and

$$\Theta^j = \int_{x_+^{j-1}}^{x_-^j} \omega(z)dz. \tag{21}$$

The key difference in our case compared to the case of $m^2\phi^2$ theory in flat background studied in [14] is that, because of the nonperiodicity of $\omega^2(x)$, the local maxima and minima of $\omega^2(x)$ increases linearly with j. This results in a nontrivial j dependence in X^j and Θ^j. Consequently, the occupation number of the $\hat{\chi}$ particles after j oscillations of the inflaton is

$$n^j_{\mathbf{k}=0} = |\beta^j|^2 = \exp\left(\sum_{\ell=1}^{j} 2X^\ell\right) \prod_{s=1}^{j} (2\cos\Theta^s). \tag{22}$$

In order to provide some useful analytical expression for $n^j_{\mathbf{k}=0}$, we need to perform some reasonable approximations in calculating the integral for X^j and Θ^j in (20) and (21). To calculate the integral in X^j we note that the bounds of integration in (20) range from $x_j^{\min} - T/4$ to $x_j^{\min} + T/4$. This suggests that as a good approximation, we can approximate $\Omega(x) = pxf(x) \simeq px_{\min}f(x)$ and the integral in (20) is approximately (for the details see Appendix A)

$$X^j = \int_{x_j^{\min}-T/4}^{x_j^{\min}+T/4} \Omega(x)dx \simeq \sqrt{px_j^{\min}} \int_{-(T/4)}^{+(T/4)} \sqrt{f(x)}dx = \sqrt{p\pi K(1/2)} \frac{\Gamma(\frac{3}{8})}{\Gamma(\frac{7}{8})} \sqrt{2j-1}, \tag{23}$$

where $\Gamma(x)$ is the gamma function and K is the complete elliptic integral of the first kind [19]. Similarly, for Θ^j

$$\Theta^j = \int_{x_j^{\max}-T/4}^{x_j^{\max}+T/4} \omega(x)dx \simeq \sqrt{px_j^{\max}} \int_{-(T/4)}^{+(T/4)} \sqrt{f(x)}dx = \sqrt{p\pi K(1/2)} \frac{\Gamma(\frac{3}{8})}{\Gamma(\frac{7}{8})} \sqrt{2j-2}. \tag{24}$$

Using the approximations proposed for harmonic number summation in Appendix B one finds $\sum_{i=1}^{j} \sqrt{2i-1} \simeq 2\sqrt{2}j^{3/2}/3$ and

$$\sum_{1}^{j} 2X^j \simeq \frac{4}{3}\sqrt{2p\pi K(1/2)} \frac{\Gamma(\frac{3}{8})}{\Gamma(\frac{7}{8})} j^{3/2}. \tag{25}$$

After j oscillations, we have $x = jT$, so for large j the exponent for $n_{\mathbf{k}=0}$ in (22) behaves as

$$n^j_{\mathbf{k}=0} \propto \exp(0.490\sqrt{p}x^{3/2}). \tag{26}$$

Quite interestingly, the occupation number grows exponentially with the exponent proportional to $x^{3/2}$. One can trace

the nonlinear exponential enhancement of the occupation number to the explicit breaking of the periodicity of $\omega^2(x)$ in (13). This is in contrast to conventional model of preheating where the source term is periodic and the Floquet theorem applies with the result that the occupation number has a linear exponential growth. One can check that the breaking of periodicity in our case is a direct consequence of conformal invariance breaking via trilinear interaction in an expanding background.

A plot of $n_{\mathbf{k}=0}$ is shown in the left graph of Fig. 2 containing the full numerical solutions and our analytical results. Although the nonlinear exponential growth captures very well the overall behavior of $n_{\mathbf{k}=0}$, the figure from the exact numerical solution shows some small wiggles and ripples which cannot be captured by the exponential profile. To take these minor but interesting discrepancies into account, we should also add the effects of the phase term originated from the products of cosines in (22). As one can see in Fig. 2 this term is oscillatory but not periodic which can explain the small oscillations in the profile of $\ln n_{\mathbf{k}=0}$ versus x. Taking the effect of the phase term into account, one obtains

$$n^j_{\mathbf{k}=0} \simeq \exp\Big[0.490\sqrt{p}x^{3/2} + \sum_{\ell=1}^{j} \ln(4\cos^2(7.427\sqrt{p\ell}))\Big], \tag{27}$$

where $j = x/T$.

In the right graph of Fig. 2 we have plotted $n_{\mathbf{k}=0}$ for different values of p. As this graph shows, with the addition of the effects of the phases, our analytical result (27) shows a perfect agreement with the exact numerical results, confirming that our analytical solution captures the correct p dependence. As one expects, the larger the value of p is, the stronger is tachyonic resonance from trilinear interaction.

B. Tachyonic resonance with $\kappa^2 \neq 0$

After presenting the analysis for the simple zero-momentum case, in this section we present the analysis for arbitrary momentum, $\kappa^2 \neq 0$. As can be seen from Fig. 1, for $\kappa^2 \neq 0$ there is no tachyonic resonance from the beginning where $\kappa^2 > px$. After some oscillations $\omega^2(x)$ becomes negative for $x \geq p/\kappa^2$ and our previous methods for tachyonic resonance would apply. From (13), we see that the frequency of oscillations becomes tachyonic after $j = j_*$ oscillations where

$$j_* = \Big[\frac{\kappa^2}{pT} + \frac{1}{2}\Big]. \tag{28}$$

Here $[z]$ represents the integer part of z.

For small x there is no tachyonic region from the start of preheating, but if the frequency becomes nonadiabatic one should expect particle production via parametric resonance as in conventional preheating analysis. However, as we shall see from our full numerical results, the particle creation from the nontachyonic scattering for $j < j_*$ oscillations is quite negligible compared to tachyonic resonance particle creation after $j > j_*$ oscillations. The nonadiabaticity condition $|\omega'(x)|/\omega(x)^2 \gg 1$ is satisfied for

$$j \geq j_{\rm nad} \simeq j_* - \frac{0.8472}{\pi\sqrt{pT}}\sqrt{j_*} \simeq j_* - \frac{0.1}{\sqrt{p}}\sqrt{j_*}. \tag{29}$$

This indicates that $j_{\rm nad} - j_* \sim$ few and the onset of parametric resonance is actually around j_* where tachyonic resonance starts. Besides the very short period of parametric resonance, the "effective" Floquet index during this

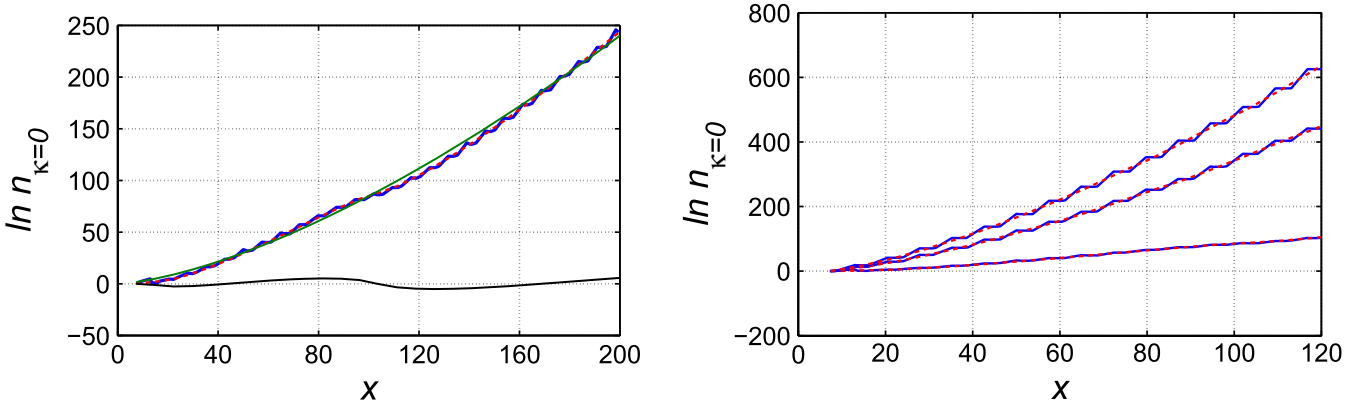

FIG. 2 (color online). Occupation number $\ln n_{\mathbf{k}=0}$ as a function of conformal time x. In the left figure with $p = 0.03$, the wavy solid curve (blue) shows the exact numerical solution, the smooth growing curve (green) shows the analytic solution (26) which does not contain the interference term, the dash-dotted curve (red) shows the analytic solution (27) which includes the interference term added and the bottom solid curve (black) shows the behavior of the interference term. In the right figure, $\ln n_{\mathbf{k}=0}$ is plotted for different values of p. Again the solid curves (blue) show the exact numerical solutions of (11) while the dashed curves (red) show the analytic solution (27). The graphs from bottom to top, respectively, correspond to $p = 0.03$, $p = 0.5$, and $p = 1$. The agreement between the full numerical results and our analytical formula, (27), is impressive.

period is much smaller than that of the tachyonic regions. Therefore, the particle production is mainly concentrated in the tachyonic regions. This result is also verified in our numerical investigations.

Repeating the same methods as in the previous section, for $j > j_*$, the Bogoliubov coefficients before and after jth oscillations are related by

$$\begin{pmatrix} \alpha_{\mathbf{k}}^{j+1} \\ \beta_{\mathbf{k}}^{j+1} \end{pmatrix} = e^{X_{\mathbf{k}}^j} \begin{pmatrix} 1 & ie^{2i\theta^j} \\ -ie^{-2i\theta^j} & 1 \end{pmatrix} \begin{pmatrix} \alpha_{\mathbf{k}}^{j} \\ \beta_{\mathbf{k}}^{j}, \end{pmatrix}, \tag{30}$$

where

$$X_{\mathbf{k}}^j \simeq \sqrt{px_j^{\min}} \int_{x_j^-}^{x_j^+} \sqrt{|r_j^{\min} + f(z)|}dz, \tag{31}$$

with $r_j^{\min} \equiv \kappa^2/px_j^{\min}$ and θ^j is the total phase accumulated from x_0 to x_j^- during the intervals where $\omega^2 > 0$. We have $\theta^j = \theta^0 + \sum_j \Theta^j$ with

$$\Theta^j \simeq \sqrt{px_j^{\max}} \int_{x_{j-1}^+}^{x_j^-} \sqrt{r_j^{\max} + f(z)}dz, \tag{32}$$

where $r_j^{\max} \equiv \kappa^2/px_j^{\max}$.

Similar to the analysis resulting in (25) and using the formulas presented in Appendix D, one obtains

$$\sum_{j_*+1}^{j} 2X_{\mathbf{k}}^{\ell} \simeq \sum_{\ell=j_*+1}^{j} \left(2a\sqrt{\frac{pT}{2}}\sqrt{2\ell-1} - 2b'\kappa^2\sqrt{\frac{2}{pT}}\frac{1}{\sqrt{2\ell-1}}\right)$$
$$\simeq \frac{4a}{3}\sqrt{pT}(j^{3/2} - j_*^{3/2}) - 4b'\kappa^2\sqrt{\frac{1}{pT}}(j^{1/2} - j_*^{1/2}) \tag{33}$$

$$\prod_{j_*+1}^{j}(2\cos\Theta_{\mathbf{k}}^j)^2 = \exp\Big[\sum_{j_*+1}^{j} \ln\Big(4\cos^2\Big(a\sqrt{pT}\sqrt{j-1} + \frac{b\kappa^2}{\sqrt{pT}}\frac{1}{\sqrt{j-1}}\Big)\Big)\Big], \tag{34}$$

where (B2) and (B3) have been used and

$$a = 2.72, \qquad b' = 2.86, \qquad b = 3.75. \tag{35}$$

After jth oscillations, $x = jT$, and the occupation number is given by

$$n_{\mathbf{k}}^j \sim \exp\left(\frac{4a\sqrt{p}}{3T}(x^{3/2} - x_*^{3/2}) - \frac{4b'\kappa^2}{\sqrt{pT}}(x^{1/2} - x_*^{1/2})\right) \times \text{interference term}, \tag{36}$$

where $x_* \equiv j_*T$ and the interference term is the expression (34).

As in the zero-momentum example, the occupation number has a nonlinear exponential dependence with the leading exponents being $x^{3/2}$ and $x^{1/2}$ respectively. The fact that before the tachyonic regions, i.e. for $x < x_*$, there is no particle creation is clearly seen in (36). Both of these two nontrivial results are a consequence of the violation of the periodicity in the resonance source term. The left plot in Fig. 3 compares our analytical result (36) with the full numerical results. The agreement is again impressive.

The interference term in (36) has a very interesting effect. Suppose for the moment that we do not take into account the interference term in (36). Since $b' > 0$, from the exponential term one may expect that the larger the value of κ^2, the more suppressed will the particle creation be. Our numerical investigations supports this general rule,

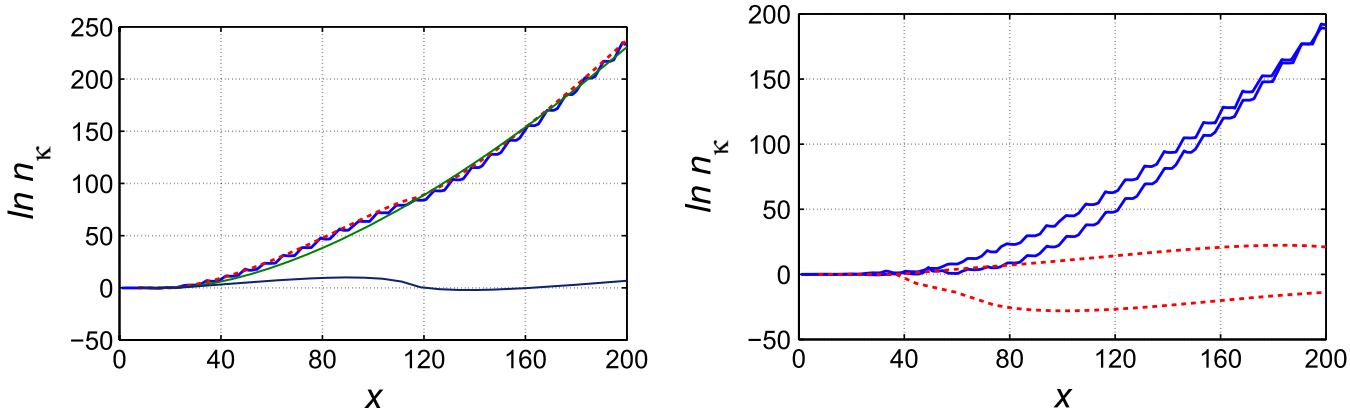

FIG. 3 (color online). The left figure shows $\ln n_{\mathbf{k}}$ as a function of x for $p = 0.05$ and $\kappa^2 = 1$. The wavy solid (blue) curve shows the exact numerical solution of (11). The (red) dashed curve shows the analytical solution (36). The smooth (green) solid curve shows the analytical solution without taking into account the interference term. The bottom (black) solid curve shows the effect of the interference term (34). The agreement between the full numerical result and the analytical formula (36) is impressive. The right figure shows the destructive effects of the interference term in (36). The lower and upper wavy (blue) solid curves show the exact numerical results for $\kappa^2 = 2$ and $\kappa^2 = 1.5$, respectively, with $p = 0.05$. The lower and upper dashed (red) curves show the effects of the interference term, for $\kappa^2 = 2$ and $\kappa^2 = 1.5$, respectively. We see that the interference term causes a suppression of particle production for $\kappa^2 = 1.5$.

but there are some noticeable exceptions. In the right graph of Fig. 3 we have presented an example where a larger κ^2 has a higher occupation number than a smaller κ^2. The resolution to this apparent paradox relies on the destructive effects of the interference term. Looking into the form of the interference term (34) one observes that the interference becomes destructive in a region in $\kappa^2 - j$ space where $\cos(\Theta^j_{\mathbf{k}})$ vanishes. For the latter, one requires the phase term $\Theta^j_{\mathbf{k}}$ to be stationary on its roots, i.e. $\cos(\Theta^j_{\mathbf{k}}) = \partial_j \Theta^j_{\mathbf{k}} = 0$ at some stationary time j_s. From (34) one easily finds that the stationary points of $\Theta^j_{\mathbf{k}}$ occur at

$$j_s = 1 + \frac{b\kappa^2}{apT}, \tag{37}$$

with

$$\Theta^{j_s}_{\mathbf{k}} = 2\sqrt{ab}\kappa. \tag{38}$$

As explained above, demanding that $\Theta^{j_s}_{\mathbf{k}} \to (2n-1)\frac{\pi}{2}$ for some integer n, one obtains the value of κ where the destructive feature of the interference term is pronounced

$$\kappa_{\text{stab}} = \frac{(2n-1)\pi}{4\sqrt{ab}} \simeq 0.25(2n-1), \qquad n = 1, 2 \ldots. \tag{39}$$

Note that $\Theta^{j_s}_{\mathbf{k}}$ and κ_{stab} are independent of p. Note also that the stable bands are equally spaced in the momentum space. It is worth checking this equation for some n. For example for $n = 2$, 3, 4, and 5, one finds $\kappa^2 = 0.54$, 1.51, 2.96, and 4. 89, respectively.

Figure 4 shows behavior of $\Theta^j_{\mathbf{k}}$ as a function of number of oscillations for three given values of κ^2. As is seen in the left and right figures the stationary point of $\Theta^{j_s}_{\mathbf{k}}$ can be near $(2n-1)\pi/2$ which causes particle production suppression.

One also observes that the destructive phase in the interference term is not static in time. This is somewhat similar to stochastic resonance phenomena observed in resonance preheating in an expanding background [1]. However, in contrast to the stochastic resonance, in our case the interference term is not completely stochastic and one can keep track of the phase at each oscillation period. The value of κ around κ_{stab}, where the destructive effects of the interference term is significant, form *semistability bands*. These semistability bands, as indicated in (37), occur at

$$x_{\text{stab}} = T + \frac{\pi^2}{16a^2p}(2n-1)^2 \simeq 7.416 + 0.0834\frac{(2n-1)^2}{p}. \tag{40}$$

A plot of the effects of the interference terms is shown in Fig. 5 with $p = 0.05$. As an example of the evolution of the semistability band consider the line $\kappa^2 = 1.5$ which corresponds to $n = 3$ in (39). For small x, the interference term has a destructive contribution. As the time goes by, effects of the interference term would become milder and less important. As explained above, for this reason we may call $\kappa^2 = 1.5$ a semistable band rather than a stable band. As shown above, the other semistable band is at $\kappa^2 \simeq 2.96$. The tachyonic resonance for this case would start at $x_* = j_* T \simeq 60$. Nonetheless, as depicted in the right graph in Fig. 5 particle creation is negligible until $x \simeq 100$; compatible with $x_{\text{stab}} \simeq 90$ obtained from (40) for $n = 4$. This is a consequence of the semistability band for $\kappa^2 = 2.96$ which suppresses the particle creation at early time and eventually loses its importance as the Universe expands further.

C. Expanding vs nonexpanding background

In the last two subsections the effects of expanding background were included in the preheating analysis via the conformal transformations $\varphi = a(\eta)\phi$ and $\hat{\chi} = a(\eta)\chi$. One consequence of the expanding background was the appearance of the nonperiodic factor x in $\omega(x)$.

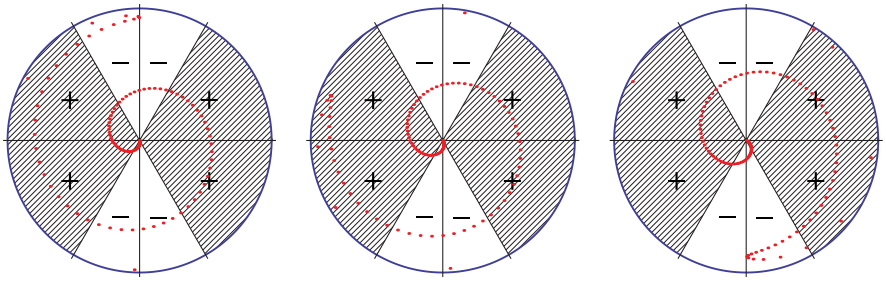

FIG. 4 (color online). Phase accumulated through j oscillations for different values of κ^2: left, $\kappa^2 = 1.51$; middle, $\kappa^2 = 2$; and right, $\kappa^2 = 2.96$. The angular position of each (red) dot indicates the value of $\Theta^j_{\mathbf{k}}$. The outer points correspond to smaller value of j and as j increases the dots move toward the center and become denser, as can be seen from the form of $\Theta^j_{\mathbf{k}}$ given in (34). As Θ^j_k tends to $(2n-1)\pi/2$, the contribution of jth oscillation in the interference term suppresses the particle production. For $\kappa = 1.51$ (left) the stationary point of Θ^j_k is near $\pi/2$. For $\kappa = 2$ (middle) the stationary point is far away from the poles, and for $\kappa = 2.96$ (right) the stationary point is near $3\pi/2$. This explains why $\kappa^2 = 1.51$ and $\kappa^2 = 2.96$ belong to the "semistability bands." Note that $\ln|2\cos\Theta^j_{\mathbf{k}}|$ is positive for $|\Theta^j_k - n\pi| < \pi/3$ and is negative for $|\Theta^j_k - (2n+1)\pi/2| < \pi/6$, which are separated in this figure by + and − signs.

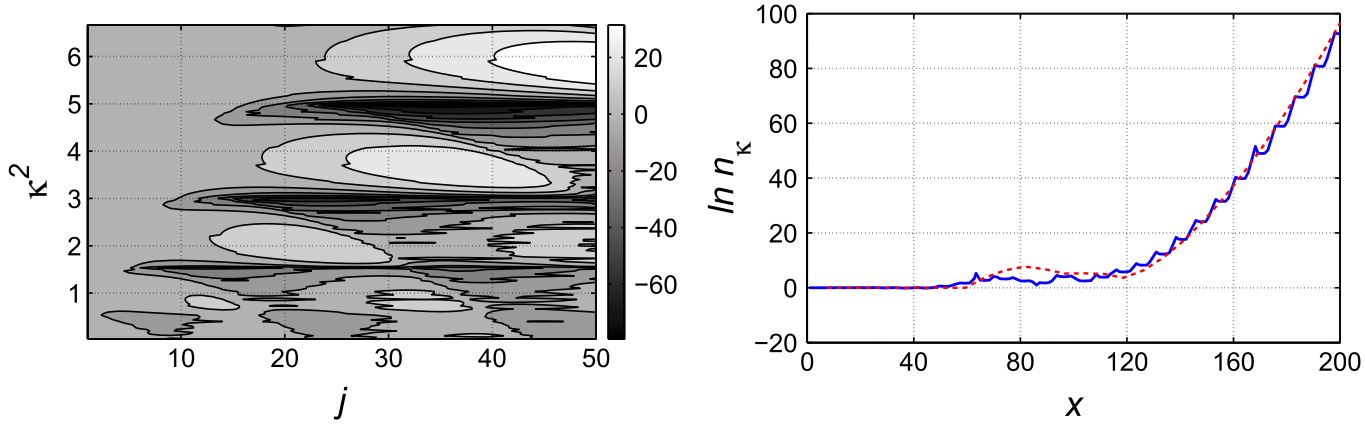

FIG. 5 (color online). In the left figure the contour plot of the phase term in $\kappa^2 - j$ plane is shown. The darker regions show the semistability bands in which the interference term suppresses particle creation. The right bar represents $\ln|2\cos\Theta^j|$ as a function of number of oscillations j. An important point of our analysis is that the semistability regions are independent of p. In the right figure, $\ln n_{\mathbf{k}}$ as a function of conformal time for the predicted semistability band $\kappa^2 \simeq 3$ is shown. The (blue) solid line shows the full numerical solutions and the (red) dashed curve shows our analytical result (36). As we predicted, particle production for this momentum is suppressed for small times because of the interference term.

This in turn leads to a nonlinear exponential particle creation. This should be compared with preheating with four-legs interaction, $g^2\phi^2\chi^2$, in $\lambda\phi^4/4$ theory which preserves the conformal invariance and $\omega^2(x)$ is periodic and one obtains a linear exponential particle creation. One may ask what would be the situation if one considers preheating with trilinear interaction in a nonexpanding flat background. The trilinear term in a flat background is periodic and, as a consequence of the Floquet theorem, one obtains a linear exponential particle creation. This seems paradoxical, noting that the expansion of the Universe usually suppresses the particle creation. As we show below, the root of this apparent paradox relies on the difference between conformal time x and the cosmic comoving time t.

In a flat background with $a(t) = 1$, the solution to the inflaton field is $\phi = \tilde{\phi} f(z)$ where $\tilde{\phi}$ is the initial amplitude of the inflaton field at the start of preheating and $f(z)$ is the Jacobi elliptic cosine function. Here we defined the dimensionless times $z \equiv \sqrt{\lambda}\tilde{\phi}t$. The equation of motion for the resonant field χ is

$$\frac{d^2\chi_{\mathbf{k}}}{dz^2} + (\kappa^2 + px_0 f(z))\chi_{\mathbf{k}} = 0, \tag{41}$$

with $x_0 = \sqrt{3/2\pi}(M_{\rm p}/\tilde{\varphi})$ and $\kappa^2 = k^2/\lambda\tilde{\varphi}^2$.

Following the same methods as in the last two subsections, the occupation number is

$$n_k^j = \exp(2jX_k)(2\cos\Theta_k)^{2(j-1)}, \tag{42}$$

with the crucial difference that now X_k is j-independent as in [14]. To a good approximation, one has

$$X_k \simeq a\sqrt{px_0} - \frac{b'}{\sqrt{px_0}}\kappa^2, \quad \text{and} \quad \Theta_k = a\sqrt{px_0} + \frac{b}{\sqrt{px_0}}\kappa^2, \tag{43}$$

where the numeric coefficients a, b, b' have the same values as before, given in (35). By substituting $j \to \tau/T$, where T is the period of oscillations of $f(z)$ (9), the occupation number of the $\mathbf{k}$ mode becomes

$$n_{\mathbf{k}}^j = \exp\left(\frac{2X_{\mathbf{k}}\sqrt{\lambda}\tilde{\phi}}{T}t\right) \times \text{interference term}. \tag{44}$$

As expected $n_{\mathbf{k}}$ has a linear exponential growth in terms of t. To compare it with the particle creation in an expanding background, we recall that in our case $t \propto x^2$ [cf. (7)] and hence (44) gives $\ln n_{\mathbf{k}} \sim x^2$ for the flat background. This confirms the intuition that in general the particle creation via tachyonic resonance is more enhanced in a flat background compared to that of an expanding background. This is understandable because the expansion of the Universe dilutes the previously produced particles and also reduces the amplitude of the source term $\phi(t)$. One should, however, note that due to the nontrivial dynamics of the interference term, this intuition may not work and for some specific regions in the κ space expansion of the Universe may enhance the particle production rate. As explained in previous subsection, the interference term is time-dependent which means the stable or unstable bands vary in time. As an example, Fig. 6 shows cases in which the particle production is more efficient in an expanding background.

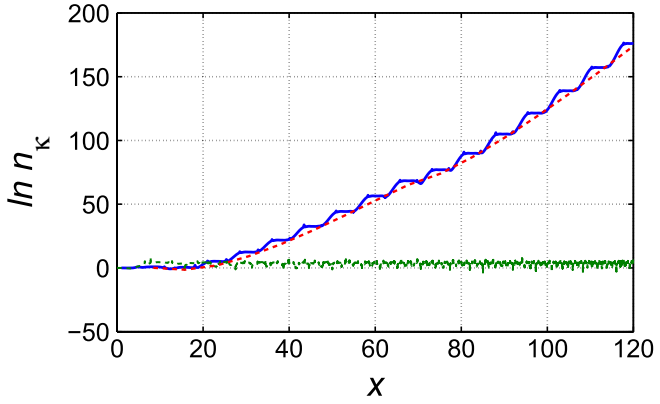

FIG. 6 (color online). Comparison between particle creations in flat and expanding backgrounds in $\lambda\phi^4/4$ theory. For $p = 0.1$ and $\kappa^2 = 0.54$, which is in a tachyonic region in a flat background, because of the effect of the interference term (43), there is no particle production for these parameters. Nonetheless, due to nonstatic interference term, there is particle production in an expanding universe. The wavy (blue) solid curve indicates the full numerical solution for an expanding universe, the (red) dashed curve shows our analytical solution, and the straight (green) line at the bottom represents the particle creation in a flat background.

III. TACHYONIC RESONANCE IN $m^2\phi^2/2$ THEORY

The $\lambda\phi^4/4$ inflationary model has the conformal symmetry and the effects of the expanding background can be incorporated by the conformal transformations $(\phi, \chi) \rightarrow a(\eta)(\phi, \chi)$. This trick does not apply to the $m^2\phi^2/2$ model and the effect of expansion should be taken care of accordingly. The analysis of the tachyonic resonance for the $m^2\phi^2/2$ model in a flat background has been studied in [14] with some brief discussions on the effects of expanding background. Here we study the tachyonic resonance for $m^2\phi^2/2$ inflationary potential in an expanding background in more detail and demonstrate that it can have very nontrivial consequences.

We start with the potential

$$V(\phi) = \frac{m^2}{2}\phi^2 + \frac{\sigma}{2}\phi\chi^2 + \frac{\lambda}{4}\chi^4, \tag{45}$$

with $\lambda > \sigma^2/2m^2$ [14]. The equation for the production of χ particles obeys

$$\hat{\chi}_k'' + (A_k + 2q\cos 2z)\hat{\chi}_k = 0, \tag{46}$$

where $\hat{\chi} = a(t)^{3/2}\chi$ and

$$mt \equiv 2z - \frac{\pi}{2}, \qquad A_k = \frac{4k^2}{m^2a^2} \equiv \frac{A_0^k}{a^2} \quad \text{and} \quad q = \frac{2\sigma\Phi_0}{m^2a^{3/2}} \equiv \frac{q_0}{a^{3/2}}. \tag{47}$$

Here prime denotes derivatives with respect to coordinate z and A_0 and q_0 indicate the values of the corresponding quantities in a flat background. For the quadratic potential, the background Universe during preheating evolves like matter domination and $a(t) = a_0(t/t_0)^{2/3}$ and in our conventions we choose $a_0 = 1$ and $t_0 = 1$.

One can incorporate effects of expansion in the tachyonic resonance analysis as follows. The tachyonic regions of (46) are centered around the minimum of $\omega^2(z)$, at $t_j = (j - 1/2)\pi$ with the scale factor $a_-(t_j) = ((j - 1/2)\pi)^{2/3}$ whereas the nontachyonic regions are centered around the maximum of $\omega^2(z)$, at $t_j = (j - 1)\pi$ with the scale factor $a_+(t_j) = ((j - 1)\pi)^{2/3}$. Following the same steps as in Sec. II A the occupation number is given by

$$n_{\mathbf{k}}^j = |\beta_{\mathbf{k}}^j|^2 = \exp\Big(\sum_{j_*+1}^{j} 2X_{\mathbf{k}}^j\Big)\prod_{j_*+1}^{j}(2\cos\Theta_{\mathbf{k}}^j), \tag{48}$$

where j_* is defined as the last nontachyonic oscillation after which tachyonic resonance starts

$$j_* = \Big[\frac{1}{\pi}\Big(\frac{A_k^0}{2q_0}\Big)^3 + \frac{1}{2}\Big], \tag{49}$$

where $[z]$ represents the integer part of z.

Using results of [14], one finds

$$X_k^j = -\frac{\alpha A_k^0}{\sqrt{q_0}a_-(t_j)^{5/4}} + 2\alpha\frac{\sqrt{q_0}}{a_-(t_j)^{3/4}} = -\frac{\alpha A_k^0}{\sqrt{q_0}t_j^{5/6}} + 2\alpha\frac{\sqrt{q_0}}{t_j^{1/2}}, \tag{50}$$

in which $\alpha = 0.85$ and $t_j = \pi(j - 1/2)$. Furthermore, the phase accumulation is given by

$$\Theta_k^j = \sqrt{\frac{q_0}{a_+(t_j)^{3/2}}}\Big[a + b\frac{A_k^0}{2q_0a_+(t_j)^{1/2}} + c\Big(1 - \frac{A_k^0}{2q_0a_+(t_j)^{1/2}}\Big)\ln\Big(1 - \frac{A_k^0}{2q_0a_+(t_j)^{1/2}}\Big)\Big], \tag{51}$$

where $a = 1.69$, $b = 2.31$, and $c = 0.46$ [14].

Using the approximations in Appendix. B for the harmonic sums, we obtain

$$\sum_{j_*+1}^{j} 2X_k^j \simeq \frac{8\alpha}{\pi}\sqrt{q_0}((j\pi)^{1/2} - (j_*\pi)^{1/2}) - \frac{12\alpha A_k^0}{\pi\sqrt{q_0}}((j\pi)^{1/6} - (j_*\pi)^{1/6}). \tag{52}$$

Finally, by substituting $j\pi \rightarrow t$ after jth oscillation, the occupation number as a function of time is

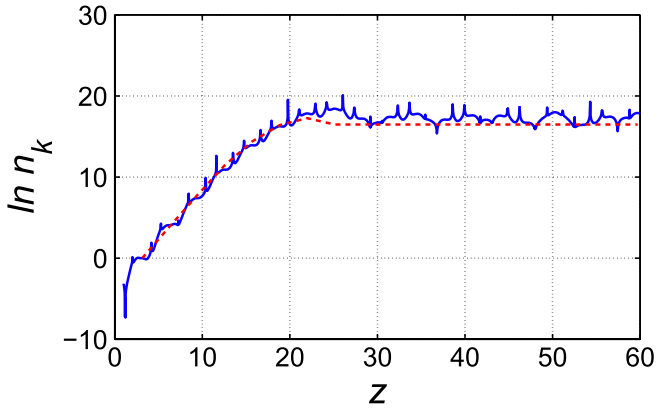

FIG. 7 (color online). The logarithm of the occupation number as a function of time for $A_k^0 = 20$ and $q_0 = 13$. The wavy (blue) curve shows the full numerical solution. The (red) dashed curve shows our analytical result (53). As expected from (54), there is no particle production after $t = 23$.

$$n_j \simeq \exp\left[\frac{8\alpha}{\pi}\sqrt{q_0}(t^{1/2} - t_*^{1/2}) - \frac{12\alpha A_k^0}{\pi\sqrt{q_0}}(t^{1/6} - t_*^{1/6})\right] \times \prod_{j_*}^{j}(2\cos\Theta_{\mathbf{k}}^j), \quad (53)$$

where $\Theta_{\mathbf{k}}^j$ is given by (51) and $t_* = j_*\pi$.

Because of the expansion of the Universe, both q and $A_{\mathbf{k}}$ decrease as t increases, but $A_{\mathbf{k}}$ decreases faster. On the other hand, the WKB approximation is valid for $2q - A > 2\sqrt{q}$ which quickly reduces to $2q > 2\sqrt{q}$. This condition is not satisfied for $q < 1$. As a result, the expansion of the Universe spoils our approximation and that is why the analytical solutions are not as precise as in the case of $\lambda\phi^4/4$ theory. As one can see from the numerical results in Fig. 7, particle production is stopped after some oscillations because of the expansion of the Universe.

In order to interpret this effect note that by reducing A_k and q, the solutions of Mathieu equation converge to the stability bands. Therefore, in the expanding background when the $A_k - q$ curve crosses the stability bands, the particle production switches off. From the stability/instability charts of Mathieu equation [19] one finds that preheating ends when

$$\frac{q_0}{t_{\rm end}} \simeq 0.8126\left(1 - \frac{A_k^0}{t_{\rm end}^{4/3}}\right). \quad (54)$$

As a result, for initial conditions with $A_k^0 > 2q_0$, there can be particle production only if $t_* > t_{\rm end}$. This does not take into account the effects of backreaction which will be studied in the next section.

As already mentioned, the expansion of the Universe dilutes the previously produced particles as well as reducing $\phi(t)$ as the source of resonance. As a result the resonance in an expanding Universe is expected to be less efficient than the nonexpanding background. More investigation shows, however, that for some specific modes $\mathbf{k}$ the expansion of Universe can actually enhance the preheating! There are two effects which can enhance particle production in an expanding background. First and less important is the k^2/a^2 term in preheating Eq. (46). The expansion of the Universe with the effect of $k^2 \to k^2/a(t)^2$ can reduce the energy cost of producing particle (but there is a trade-off between this effect and the effects of diluting ϕ condensate and the reduction of the source term). Second and the more important is the effect of varying interference term in an expanding background.

We first focus on the former effect. The occupation number in a flat background is given by [14]

$$n_{\mathbf{k}}^j \simeq \exp\left[2j\left(2\alpha\sqrt{q_0} - \frac{\alpha}{\sqrt{q_0}}A_k^0\right)\right](2\cos\Theta_{\mathbf{k}})^{2(j-1)}, \quad (55)$$

where

$$\Theta_k = \sqrt{q}\left[a + b\frac{A_k}{2q} + c\left(1 - \frac{A_k}{2q}\right)\ln\left(1 - \frac{A_k}{2q}\right)\right]. \quad (56)$$

As one can expect from the Floquet theorem, the occupation number has a linear exponential growth with time (or number of oscillations) in a flat background. Compare this with our result (53) where the occupation number grows with an exponent which scales like $t^{1/2}$ or $j^{1/2}$. In general this leads to the conclusion that at large t the tachyonic resonance is less efficient in the expanding background as compared to the flat background. For the intermediate times the situation could be different. To see this note that the second term in the big bracket in (53), which suppresses the particle creation, scales like $t^{1/6}$ in an expanding background whereas it scales linearly with t in a flat background. This difference in scaling results in an enhancement of particle creation for some certain modes in an expanding background. However, after some oscillations the second terms in brackets in (53) and (55) become negligible compared to the first terms in the corresponding brackets. Approximately this occurs for $t \sim 30t_*$ and particle production in an expanding background becomes more and more inefficient compared to the static Universe. One can see this feature for $q_0 = 125$ and $A_k^0 = 230$ in Fig. 8, showing that the particle production in an expanding background is more efficient for about the first 60 oscillations.

As mentioned above the interference term can play an important role in relative enhancement of particle production in an expanding background. In the stability/instability chart of the Mathieu equation there are vast regions where there is no particle production due to destructive interference term. However, as we described at the end of subsection II B, in an expanding background the phase term is not static and is varying with time. As such and as time advances, the solutions in the stability bands can escape from the stability bands. Inside the tachyonic re-

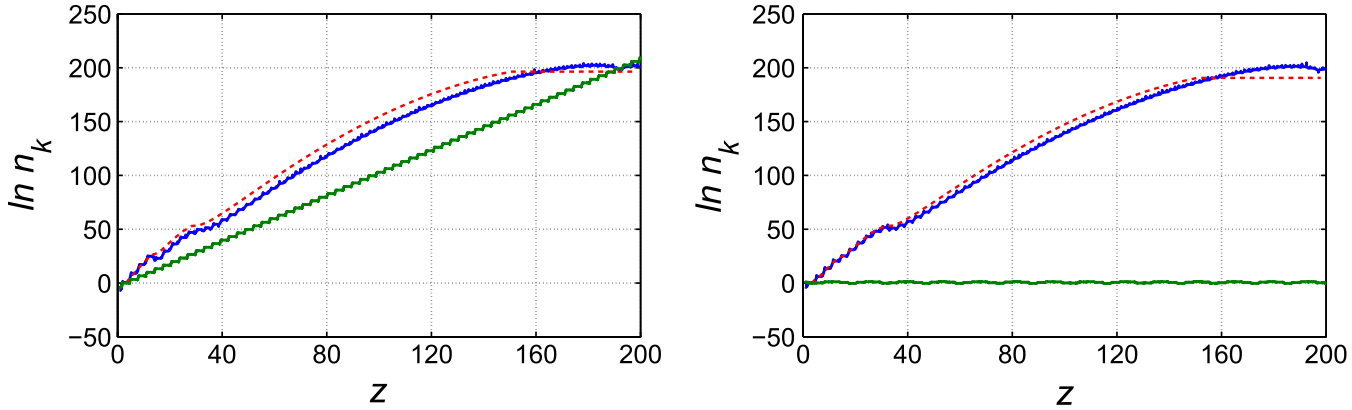

FIG. 8 (color online). Left: the logarithm of the occupation number as a function of time for $A_k^0 = 230$ and $q_0 = 125$. It shows that the expansion of the Universe can enhance the particle creation by reducing the energy cost of particle production via $k^2 \to k^2/a^2(t)$. The solid curve (blue) shows our full numerical result in an expanding universe. The lower straight solid line (green) shows numerical results for a nonexpanding universe. The dashed curve (red) shows our analytical results in an expanding background (53). Right: logarithm of the occupation number for $A_k^0 = 260$ and $q_0 = 125$. This figure shows that because of the time-varying nature of the interference term, the solutions can escape from the stability bands. The solid curve (blue) represents our full numerical result in an expanding universe. The bottom solid line (green) shows the numerical results for a nonexpanding universe. The dashed curve (red) shows our analytical solution in an expanding background (53).

gion, far from $A_k = 2q$ line, the effect of phase term is suppressed, but by going toward the line $A_k = 2q$ the stable regions are formed. So, in a flat background there is no particle creation in this region but as described above, in an expanding background, the solutions can escape these stability bands, leading to an enhancement in particle creation (see the right graph in Fig. 8).

IV. BACKREACTION OF χ PARTICLES AND END OF PREHEATING

So far we have neglected the backreactions of the produced particles on classical background ϕ and on χ particles occupation number. There are important effects which can change this simple picture. We classify these effects by the form of their interactions.

First, trilinear interaction at one-loop Hartree approximation contributes as a source term in ϕ equation of motion. This leads to a nonzero vacuum expectation value for ϕ which is expected, because as one can see from (1), the minimum of the potential is located at a nonzero value of ϕ. Second, the self-interaction of χ particles can increase the effective mass of χ particles. This effect can make χ particles so heavy that they cannot be produced through interaction with ϕ, terminating the preheating.

A. Backreaction in $\lambda\phi^4$ theory

Let us first ignore the effects of decay of inflaton field through trilinear interaction and consider the inflaton field as a background field. The preheating is complete if all the energy from the background field ϕ is transferred into created χ particles. One can estimate the energy in the χ particles as

$$\rho_\chi = \frac{1}{a^2(x)} \int \frac{d^3k}{(2\pi)^3} |\omega_k| n_k^\chi. \tag{57}$$

The $1/a^2$ factor in front of the integral has appeared because we are working in the conformal frame and that $\rho_{\rm conf} = \rho_{\rm comoving}/a^2$. Note also that $n_k^\chi = n_{\mathbf{k}}^j/a^2(x)$, with $n_{\mathbf{k}}^j$ given in (36). The integral over k is cut off at $k_{\rm max}^2 \lesssim \lambda\tilde{\varphi}^2 px$. This upper bound comes from the fact that for a given time x particle creation starts for $x > x_*$, which in turn, recalling (28), implies the bound mentioned above.

In the conformal frame, at one-loop Hartree approximation, the dispersion relation is

$$\omega_{\mathbf{k}}^2 = \lambda\tilde{\varphi}^2 \left(\kappa^2 + pxf(x) + 3\frac{\lambda'}{\lambda} \frac{\langle \hat{\chi}^2 \rangle}{\tilde{\varphi}^2} \right), \tag{58}$$

and for our estimate of ρ_χ at this stage, we drop the last term and justify this approximation later on in this subsection. Moreover, for the period when the particle creation is more pronounced one may also drop the κ^2 term and approximate ω^2 by $\lambda\tilde{\varphi}^2 pxf(x)$ or

$$\omega \simeq \sqrt{\sigma a(x)|\varphi(x)|}. \tag{59}$$

With this approximation

$$\rho_\chi = \frac{1}{a^4(x)} |\omega| \int \frac{d^3k}{(2\pi)^3} n_k^j \equiv \frac{1}{a^4(x)} n_\chi |\omega|, \tag{60}$$

where[3]

[3]Here $a = 2.72$, as given in (35), and should not be mistaken with the scale factor $a(x)$.

$$n_\chi \approx \int_0^{k_{\max}} \frac{d^3k}{(2\pi)^3} \exp\Big(\frac{4a\sqrt{p}}{3T}(x^{3/2} - x_*^{3/2}) - \frac{4b'\kappa^2}{\sqrt{p}T}(x^{1/2} - x_*^{1/2})\Big) \quad (61)$$

is the total number of χ particles produced. In order to perform the above integral we note that it could be written in the form

$$n_\chi \approx \frac{e^{\zeta\sqrt{p}x^{3/2}}}{2\pi^2}(\lambda\tilde{\varphi}^2)^{3/2}\int_0^{\sqrt{px}} d\kappa\kappa^2 e^{A\kappa^3 - B\kappa^2}, \quad (62)$$

where $\zeta = 4a/(3T) \simeq 0.5$, $A = (12b' - 4a)/3pT$, and $B = 4b'\sqrt{x}/\sqrt{p}T$. This integral cannot be calculated analytically and one should approximate it. Comparing the two terms in the exponent of the integrand

$$\frac{A\kappa^3}{B\kappa^2} = \frac{(3b' - a)}{3b'}\frac{\kappa}{\sqrt{px}} \simeq 0.7\frac{\kappa}{\sqrt{px}}, \quad (63)$$

we see that for the range of integration $\kappa < \sqrt{px}$ one can neglect term $A\kappa^3$ and just take the $-Bk^2$ term, reducing the integral to an incomplete Gaussian integral. For large values of x, which we are interested in, i.e. for $\sqrt{p}x^{3/2} \gtrsim T/b' \approx 2.6$, the integral can be computed, leading to

$$n_\chi \approx \frac{1}{64}\Big(\frac{\sqrt{p}T}{\pi b'}\Big)^{3/2}(\lambda\tilde{\varphi}^2)^{3/2}x^{-3/4}e^{\zeta\sqrt{p}x^{3/2}}. \quad (64)$$

Preheating completes at $x_{\rm cop}$, where

$$\rho_\chi(x_{\rm cop})a^3(x_{\rm cop}) \sim \rho_\phi^0 = \frac{\lambda}{4}\tilde{\varphi}^4, \quad (65)$$

which happens when

$$x_{\rm cop}^{-5/4}e^{\zeta\sqrt{p}x_{\rm cop}^{3/2}} \approx \frac{16}{\lambda p^{5/4}}\Big(\frac{\pi b'}{T}\Big)^{3/2}\sqrt{\frac{2\pi}{3}}\frac{\tilde{\varphi}}{M_P} \approx \frac{3.1}{\lambda p^{5/4}}. \quad (66)$$

As one expects by increasing p preheating shuts off sooner. This is reasonable, since the bigger the value of p, the stronger is the trilinear interaction which results in a more efficient χ particle production and a stronger backreaction effect. As an example, with $p = 0.05$ and $\lambda = 10^{-14}$, one finds $x_{\rm cop} \simeq 52.5$ which is about 7 oscillations.

As the density of χ particle grows and is seen from (58), the effective mass of χ particles also grows and production of them becomes more costly and eventually terminate the preheating. This happens at x_1, and at first loop Hartree approximation it is when

$$3\lambda'\langle\hat{\chi}^2\rangle|_{x_1} \approx \lambda p x_1\tilde{\varphi}^2. \quad (67)$$

On the other hand, the produced χ-particles also backreact on the dynamics of the inflation field $\phi(t)$ and may cause preheating to stop before completion, making our preheating model inefficient. To check when this can happen we note that backreaction of χ particles at one-loop Hartree approximation level, modifies the φ Eq. (5) to

$$\varphi'' + \lambda\varphi^3 + \frac{\sigma a(x)}{2}\langle\hat{\chi}^2\rangle = 0. \quad (68)$$

The backreaction of χ particles on φ becomes important at x_2, when

$$\sigma(a(x)\langle\hat{\chi}^2\rangle)|_{x_2} \approx 2\lambda\tilde{\varphi}^3. \quad (69)$$

Whichever of the two stopping mechanisms happens first marks the end of preheating. We will denote this time by $x_{\rm eop}$, where $x_{\rm eop} = \min(x_1, x_2)$. The condition of having a successful preheating is then $x_{\rm eop} \gtrsim x_{\rm cop}$.

To evaluate the x_1 and x_2 we note that within our approximations

$$\langle\hat{\chi}^2\rangle = \int\frac{d^3k}{(2\pi)^3}\frac{n_k^j}{|\omega_k|} \approx \frac{n_\chi}{|\omega|}, \quad (70)$$

with $|\omega|$ given in (59). This leads to

$$n_\chi(x_1) \approx \frac{1}{3\lambda'}(p\lambda x_1)^{3/2}\tilde{\varphi}^3, \quad (71a)$$

$$n_\chi(x_2) \approx 2\lambda(p\lambda x_2)^{-1/2}\tilde{\varphi}^3. \quad (71b)$$

Using n_χ given in (64) we end up with

$$x_1^{-9/4}e^{\zeta\sqrt{p}x_1^{3/2}} \approx \frac{64}{3\lambda'}\Big(\frac{\pi b'}{T}\Big)^{3/2}p^{3/4} \simeq \frac{28.51}{\lambda'}p^{3/4}, \quad (72a)$$

$$x_2^{-1/4}e^{\zeta\sqrt{p}x_2^{3/2}} \approx \frac{128}{\lambda}\Big(\frac{\pi b'}{T}\Big)^{3/2}p^{-5/4} \simeq \frac{171}{\lambda p^{5/4}}. \quad (72b)$$

As we see x_1 depends on λ' whereas x_2 depends on λ. For $\lambda \sim \lambda' \sim 10^{-14}$ and with $p = 0.05$, we find that $x_1 \simeq x_2 \simeq 52.5$. This means that for this choice of parameters $x_{\rm eop} \simeq 52.5$ which is very close to the completion of preheating time $x_{\rm cop}$ and hence we expect an efficient preheating.

Given the above expressions one may ask for which range of parameters p, λ, λ' the "efficient preheating" condition $x_{\rm eop} \gtrsim x_{\rm cop}$ is satisfied. The comparison between x_2 and $x_{\rm cop}$ is somewhat straightforward, noting that in the range of parameters that we are mainly interested in, n_χ/ω is a monotonic function of x and hence if $a(x_2) < 8$ (or equivalently $x_2 \lesssim 55$) $x_2 < x_{\rm cop}$ and vice versa. Moreover, one can argue that either $x_1^2 > U > x_2^2$ with $x_1x_2 > U$, or $x_1^2 < U < x_2^2$ with $x_1x_2 < U$, where $U \equiv 6\lambda'/(\lambda p^2)$. In the former case, the $x_{\rm eop} \gtrsim x_{\rm cop}$ condition roughly boils down to $500p^2\frac{\lambda}{\lambda'} \gtrsim 1$. In the latter case, when $x_{\rm eop} = x_1$, one may again show that a similar bound holds. This condition together with (3) specifies the range of parameters for which we have a simple slow-roll $\lambda\phi^4$ inflation as well as efficient preheating:

$$2 \times 10^{-3} \lesssim p^2\frac{\lambda}{\lambda'} \lesssim 1. \quad (73)$$

For typical $\lambda \sim \lambda'$ values, this leads to $2 \times 10^{-3} \lesssim p^2 \lesssim 1$.

It is also notable that $\sigma a(x)\langle\hat{\chi}^2\rangle \approx \frac{\sqrt{\sigma a(x) n_\chi}}{\sqrt{|\varphi|}}$ term shifts the minimum of the potential of φ from $\varphi = 0$ and we expect the end point of preheating to be not far from the $\varphi_{\min}$. As a rough estimate of this minimum value (assuming that $x_1 \sim x_2$), at this approximation level, is $\varphi^2_{\min} \approx a^2(x_2)\sigma^2/(6\lambda\lambda')$. For our estimates, where $a(x_2) \sim 8$, this rough estimate is not far from the global minimum of the potential (1) which is at $\phi_0^2 = \sigma^2/(2\lambda\lambda')$.

Before ending this subsection let us briefly discuss the production of φ particles and rescattering of χ particles in the theory with potential (1). At tree level the $\varphi_{\mathbf{k}}$ modes will be sourced by a term like $\lambda\langle\varphi^2\rangle$. This term being positive and periodic, following the discussions of [17], leads to stochastic resonant production of $\varphi_{\mathbf{k}}$ modes, which at large x, has an average exponential growth in x. This effect compared to the tachyonic resonant production of χ particles is very small and one may safely conclude that during preheating mainly χ particles are produced.

At one-loop level there is a contribution to the equation of motion for the $\hat{\chi}_{\mathbf{k}}$ mode proportional to $\lambda\sigma^2\varphi^2/k^2 \propto \lambda^2 p^2 (\frac{M_P}{k})^2 f^2(x)$. This, unlike the tachyonic source term, $pxf(x)$, is always positive. Nonetheless being proportional to $\lambda^2 p^2$, this one-loop contribution, is too small compared to the tree level $pxf(x)$ term. With the trilinear $\phi\chi^2$ coupling, produced χ particles will not backreact on the production of $\varphi_{\mathbf{k}}$ modes, at first loop level beyond the Hartree approximation, which we have already discussed. This is in contrast with the four-leg $\phi^2\chi^2$ interaction, where nonzero $\langle\chi^2\rangle$ contribute to the equation of motion of $\varphi_{\mathbf{k}}$.

B. Backreaction in $m^2\phi^2$ theory with trilinear interaction

The important point in this case is that following (54) and discussions leading to it, we note that in the $m^2\phi^2$ theory there is a definite time, $t_{\rm end}$, after which there is no particle production at all. Therefore, to have an efficient preheating the energy transfer form the ϕ background into χ particles should happen before this time.

As in $\lambda\phi^4/4$ case lets us estimate the time at which the energy transferred into the χ particles becomes comparable to the background energy. The energy density of χ particles after time t is

$$\rho_\chi = \int \frac{d^3k}{(2\pi)^3}|\omega_k| n_k^\chi = \frac{1}{a^3(t)}\int \frac{d^3k}{(2\pi)^3}|\omega_k| n_j, \qquad (74)$$

where n_j is given in (53) and from potential (45) one reads that at one-loop Hartree approximation

$$\omega_k^2 = \frac{k^2}{a^2(t)} + \frac{\sigma\varphi(t)}{(a(t))^{3/2}} + \frac{3\lambda}{a^3(t)}\langle\hat{\chi}^2\rangle = k^2 t^{-4/3} + \sigma t^{-1}\varphi(t) + 3\lambda t^{-2}\langle\hat{\chi}^2\rangle, \qquad (75)$$

with $\varphi(t) = \Phi_0 \sin mt$. The main contribution to the integral (74) comes from the period when the tachyonic resonance is at work. In this period one may drop k^2/a^2 term in (75). For the current estimation we also drop the backreaction of χ particles, to which we will return later. Therefore,

$$\omega^2 \simeq \frac{\sigma\varphi(t)}{a^{3/2}} = \sigma t^{-1}\varphi(t). \qquad (76)$$

Inserting (76) into (74) we find

$$\rho_\chi \approx \frac{1}{a^3}|\omega|\int \frac{d^3k}{(2\pi)^3} n_j \equiv \frac{1}{a^3}|\omega| n_\chi, \qquad (77)$$

where

$$n_\chi \approx \int_0^{k_{\max}} \frac{d^3k}{(2\pi)^3} \exp\Big[\frac{8\alpha}{\pi}\sqrt{q_0}(t^{1/2} - t_*^{1/2}) - \frac{12\alpha A_k^0}{\pi\sqrt{q_0}}(t^{1/6} - t_*^{1/6})\Big]. \qquad (78)$$

In the above, as in the $\lambda\phi^4$ case, the upper bound on k, $k_{\max}$, comes from the fact that particle creation becomes efficient for $t > t_* = \pi j_*$ with j_* given in (49), that is $k_{\max} \lesssim m\sqrt{\frac{q_0}{2}}t^{1/6}$. To perform the integral we note that it has the same form as in (62), with a cubic and a quadratic term in the exponent, where now $A = \frac{32\sqrt{2}\alpha}{\pi m^3 q_0}$, $B = \frac{48\alpha}{\pi m^2\sqrt{q_0}}t^{1/6}$ and hence $Ak/B \lesssim 2/3$. One may again drop the Ak^3 term and approximate the integral by an incomplete Gaussian integral

$$n_\chi \approx \frac{e^{\zeta\sqrt{q_0 t}}}{2\pi^2}\int_0^{k_{\max}} dk k^2 e^{-Bk^2} \simeq \frac{m^3 q_0^{3/4}}{512(3\alpha)^{3/2}} t^{-1/4} e^{\zeta\sqrt{q_0 t}}, \qquad (79)$$

where $\zeta = 8\alpha/\pi \simeq 2$ and in the last step we have approximated the integral for $q_0 t \gtrsim 1$.

Preheating is complete at $t_{\rm cop}$ when the energy of χ particles becomes comparable to the energy in the inflaton condensate at the beginning of preheating in the same comoving volume, i.e.

$$\rho_\chi a^3(t)|_{t_{\rm cop}} = (n_\chi|\omega|)|_{t_{\rm cop}} \approx \frac{1}{2}m^2\Phi_0^2. \qquad (80)$$

Using the expressions given above we obtain

$$t_{\rm cop}^{-3/4} e^{\zeta\sqrt{q_0 t_{\rm cop}}} \approx 256\sqrt{2}(3\alpha)^{3/2} q_0^{-5/4}\left(\frac{\Phi_0}{m}\right)^2 \simeq 1474 q_0^{-5/4}\left(\frac{\Phi_0}{m}\right)^2. \quad (81)$$

For $q_0 = 50$ and $\Phi_0/m \sim 10^5$, the above is satisfied for $t_{\rm cop} \simeq 3.5$ which is slightly more than one period time (which is $t = \pi$). In order to have an efficient preheating, we should demand that the preheating completes before the particle creation stops. The latter happens at $t_{\rm end}$ given in (54). $t_{\rm end} > t_{\rm cop}$ imposes a lower bound on q_0. For $\Phi_0/m \sim 10^5$, we find

$$q_0 > q_0^c \simeq 13. \quad (82)$$

Noting that $q_0 = 2\sigma\Phi_0/m^2$, this can be used to impose a lower bound on σ, the scale involved in trilinear coupling, $\sigma/m > 6.5 m/\Phi_0 \simeq 6.5 \times 10^{-5}$.

As $\langle\chi^2\rangle$ increases χ-particle effective mass increases, cf. (75), which in turn can stop preheating. One needs to also verify that this happens after the completion of preheating, that is

$$3\lambda t^{-2}\langle\hat{\chi}^2\rangle \lesssim \sigma t^{-1}\varphi(t) \quad (83)$$

at $t_{\rm cop}$. Noting that

$$\langle\hat{\chi}^2\rangle \approx n_\chi \frac{1}{|\omega|}, \quad (84)$$

with n_χ given in (79), $\lambda\langle\hat{\chi}^2\rangle \approx \sigma t\varphi(t)$ happens when $(q_0 t)^{-3/4} e^{\zeta\sqrt{q_0 t}} \simeq \frac{512}{3\lambda}(\frac{3\alpha}{2})^{3/2}$. The condition (83) is satisfied if $\lambda \lesssim 0.17(\frac{m}{\Phi_0})^2 q_0^2 = 0.67(\frac{\sigma}{m})^2$. Noting the condition for positivity of the potential (45), an efficient preheating scenario happens if λ is in the very tight range:

$$0.5\left(\frac{\sigma}{m}\right)^2 \le \lambda \lesssim 0.67\left(\frac{\sigma}{m}\right)^2. \quad (85)$$

For $\sigma/m \sim 10^{-4}$ (when $q_0 = 20$) that is, $5 \times 10^{-9} \le \lambda \lesssim 6.7 \times 10^{-9}$.

In the $m^2\phi^2$ case, with the potential (45), at one-loop Hartree approximation level the equation of motion for the background ϕ field is modified as

$$\ddot{\varphi} + m^2\varphi + \frac{1}{2a^{3/2}}\sigma\langle\hat{\chi}^2\rangle = 0, \quad (86)$$

where $a^{3/2} = t$, $\varphi = a^{3/2}\Phi$, and $\hat{\chi} = a^{3/2}\chi$. Using (76) and (84), we observe that the force term in (86) at the completion of preheating time can vanish for a nonzero φ, $\varphi_{\rm min}$: $m^2\varphi_{\rm min} \sim \sigma t^{-1} n_\chi/2\omega|_{t=t_{\rm cop}}$ which upon using (80) we obtain

$$m^2\varphi_{\rm min} \sim \sigma t^{-1}\frac{\frac{1}{2}m^2\Phi_0^2}{2\sigma t^{-1}\varphi_{\rm min}} = \frac{m^2\Phi_0^2}{4\varphi_{\rm min}} \quad (87)$$

or $\varphi_{\rm min} \sim \frac{1}{2}\Phi_0$. It is interesting that our rough estimates and considering the one-loop Hartree approximation reproduce the order of magnitudes of the minimum obtained in numerical analysis of [14] (see Fig. 3 in Ref. [14]).

V. SUMMARY

In this paper we have studied tachyonic resonance preheating via trilinear interaction in an expanding background. Because of the three-leg interaction the conformal symmetry in $\lambda\phi^4/4$ inflationary theory is broken. This induces a nonperiodic source term in the resonant χ field equation. Interestingly, one observes that the particle creation has a nonlinear exponential enhancement with the leading exponent $\sim x^{3/2}$. This is in contrast to particle creation via parametric resonance from the four-legs interaction in this theory which preserves the conformal invariance and a linear exponential growth of particle creation is obtained. Besides the nonlinear exponential growth, the interference term obtained from the accumulation of the phase term in nontachyonic scattering regions has a very nontrivial behavior in an expanding background. It is shown that there are ''semistability bands'' where $\partial_j\Theta_{\mathbf{k}}^{j_s} = \cos\Theta_{\mathbf{k}}^{j_s} = 0$ for some oscillations j_s. As a result, the particle creation for the corresponding modes is highly suppressed. However, due to time varying nature of the phase term, the semistability bands are washed out as time goes by.

The tachyonic resonance preheating in an expanding background for $m^2\phi^2/2$ theory was also studied. In general the expansion of the Universe suppresses the particle creation. However, due to the time-varying nature of the interference term, the expansion of the Universe can actually enhance the particle creation for certain modes.

We studied in some detail the backreaction of the χ particles on the dynamics of preheating and the background inflaton field ϕ. As we argued demanding an efficient preheating (i.e. demanding that particle production ends not before most of the energy in the background φ field is transferred into the χ particles) imposes strong bounds on the parameters of the potential in both $\lambda\phi^4$ and $m^2\phi^2$ cases.

For typical values of the parameters of the potential for $\lambda\phi^4$ theory preheating is complete and lasts for $\lesssim 10$ oscillations while for $m^2\phi^2$ in few oscillations the energy transfer to χ particles seems to be complete.

ACKNOWLEDGMENTS

We are deeply grateful to late Lev Kofman for stimulating discussions and for bringing Ref. [14] into our attention which started this project. To our great sadness, he passed away while this work was almost finished. We also would like to thank Bruce Bassett and Robert Brandenberger for useful discussions and Hesam Moosavimehr for computational assistance. H. F. would like to thank CITA and

Perimeter Institute for hospitality where this work started. A. A. would like to thank IPM and "Bonyad Nokhbegan Iran" for partial support.

APPENDIX A: PROPERTIES OF JACOBI ELLIPTIC COSINE FUNCTIONS $cn(x|m)$

Here we briefly review the properties of the Jacobi elliptic cosine function $cn(z|m)$. Note that we follow the convention of [19] which differs from the convention of [17]. A useful representation of the Jacobi elliptic cosine functions is [20]

$$cn(z|m) = \frac{2\pi}{\sqrt{m}K(m)} \sum_{n=0}^{\infty} \frac{q(m)^{n+1/2}}{1+q(m)^{2n+1}} \times \cos\left((2n+1)\frac{\pi z}{2K(m)}\right), \tag{A1}$$

where

$$q(m) = \exp\left(-\frac{\pi K(1-m)}{K(m)}\right)$$

and $K(m)$ is the complete elliptic integral of the first kind.

The Jacobi elliptic cosine is periodic with period $T = 4K(m)$ and has zeros at

$$x_j^- = \left(j - \frac{3}{4}\right)T, \qquad x_j^+ = \left(j + \frac{1}{4}\right)T. \tag{A2}$$

The minima and maxima are at

$$x_j^{\max} = (j-1)T, \qquad x_j^{\min} = \left(j - \frac{1}{2}\right)T. \tag{A3}$$

For the special case of $m = 1/2$ this formula reduces to

$$f(x) = cn\left(x|\frac{1}{2}\right) = \frac{2\sqrt{2}\pi}{K(\frac{1}{2})} \sum_{n=0}^{\infty} \frac{e^{-\pi(n+1/2)}}{1+e^{-\pi(2n+1)}} \cos\left((2n+1)\frac{\pi z}{2K(\frac{1}{2})}\right). \tag{A4}$$

As can be seen from above, $f(x)$ is even and periodic with the periodicity $T = 4K(\frac{1}{2}) = \frac{\Gamma^2(1/4)}{\sqrt{\pi}} \approx 7.416$.

APPENDIX B: APPROXIMATIONS FOR GENERALIZED HARMONIC NUMBERS

Here we present some useful formulas for the sums of the harmonic numbers which are used to calculate the sum over j for the occupation number in (25), (33), and (52).

With straightforward algebra one can check that

$$\sum_{i=1}^{j} \sqrt{i} \simeq \frac{2}{3} j^{3/2} + \frac{1}{2} j^{1/2} - \frac{1}{6}, \tag{B1}$$

$$\sum_{i=1}^{j} \frac{1}{\sqrt{i}} \simeq 2j^{1/2} + \frac{1}{2} j^{-1/2} - \frac{3}{2}, \tag{B2}$$

and

$$\sum_{i=1}^{j} \sqrt{2i-1} \simeq \frac{2\sqrt{2}}{3} j^{3/2}, \tag{B3}$$

which are numerically confirmed to have a very good accuracy.

One can generalize these approximations for arbitrary power $s \neq -1$

$$\sum_{i=1}^{j} i^s \simeq \frac{1}{s+1} j^{s+1} + \frac{1}{2} j^s + \frac{s-1}{2s+2}. \tag{B4}$$

APPENDIX C: APPROXIMATION FOR CALCULATING $\int_{x_j^{\max}-T/4}^{x_j^{\max}+T/4} \sqrt{xf(x)}dx$

In this appendix we would like to examine the approximation used in calculating the integral in (23):

$$\int_{x_j^{\max}-T/4}^{x_j^{\max}+T/4} \sqrt{xf(x)}dx \simeq \sqrt{x_j^{\max}} \int_{-(T/4)}^{+(T/4)} \sqrt{f(x)}dx. \tag{C1}$$

Defining $x = x_j^{\max} + u$, one finds

$$\int_{x_j^{\max}-T/4}^{x_j^{\max}+T/4} \sqrt{xf(x)}dx = \sqrt{x_j^{\max}} \int_{-T/4}^{T/4} \sqrt{1+\frac{u}{x_j^{\max}}} \times \sqrt{f(x_j^{\max}+u)}du = \sqrt{x_j^{\max}} \int_{-T/4}^{T/4} \sqrt{1+\frac{u}{x_j^{\max}}}\sqrt{f(u)}du. \tag{C2}$$

In the last step we have used the relation $f(x_j^{\max}+u) = f(x)$ (see Appendix A). Expanding the first square root in the integral and noting that $f(x)$ is an even function, one finds

$$\int_{x_j^{\max}-T/4}^{x_j^{\max}+T/4} \sqrt{xf(x)}dx = \sqrt{x_j^{\max}} \int_{-T/4}^{T/4} \sqrt{f(u)}du \times \left(1 + \mathcal{O}\left(\frac{1}{16(j-1)^2}\right)\right). \tag{C3}$$

For our case, we need $j > 1$, so the first correction can lead to maximum 6% error. Since the higher corrections are inversely related to square of $j-1$, the errors decay very quickly. For example for $j = 4$ the error is less than 1%.

APPENDIX D: APPROXIMATION FOR CALCULATING $\int_{x_{j-1}^+(r)}^{x_j^-(r)} \sqrt{r+f(x)}dx$ FOR $0 < r < 1$

Here we demonstrate the approximations used to calculate the integral in (31) and (32).

From (A1) one finds that

$$cn(x + x_j^{\max}|m) = cn(x|m) \quad \text{and}$$
$$cn(x + x_j^{\min}|m) = -cn(x|m). \tag{D1}$$

The function $r + f(x)$ with $0 < r < 1$ has zeros at

$$\begin{aligned} x_j^-(r) &= x_j^{\max}(r) + K\left(\arccos(-r)|\frac{1}{2}\right) \\ &= x_j^{\min}(r) - 2K\left(\frac{1}{2}\right) + K\left(\arccos(-r)|\frac{1}{2}\right) \\ x_j^+(r) &= x_{j+1}^{\max}(r) - K\left(\arccos(-r)|\frac{1}{2}\right) \\ &= x_j^{\min}(r) + 2K\left(\frac{1}{2}\right) - K\left(\arccos(-r)|\frac{1}{2}\right), \end{aligned} \tag{D2}$$

where $K(x|m)$ is the incomplete elliptic integral of the first kind with parameter m and amplitude x [19]. We propose following approximations:

$$\int_{x_{j-1}^+(r)}^{x_j^-(r)} \sqrt{r + f(x)}dx \simeq a + br, \tag{D3}$$

with $a = \sqrt{\frac{\pi}{2}}\frac{\Gamma(\frac{3}{8})}{\Gamma(\frac{7}{8})} = 2.72$, $b = 3.748$ and

$$\int_{x_j^-(r)}^{x_j^+(r)} \sqrt{|r + f(x)|}dx \simeq a - b'r, \tag{D4}$$

with $b' = 2.864$. The fact that $b' > 0$ has the important consequence that the occupation number $n_{\mathbf{k}} \neq 0$ is more suppressed for higher values of k; see subsection II B for the details.

Both of these approximations are verified numerically to a good accuracy. Of course, to have higher accuracies one can keep higher powers of r in above expansions.

[1] L. Kofman, A. D. Linde, and A. A. Starobinsky, Phys. Rev. D **56**, 3258 (1997).
[2] L. Kofman, A. D. Linde, and A. A. Starobinsky, Phys. Rev. Lett. **73**, 3195 (1994).
[3] J. H. Traschen and R. H. Brandenberger, Phys. Rev. D **42**, 2491 (1990).
[4] Y. Shtanov, J. H. Traschen, and R. H. Brandenberger, Phys. Rev. D **51**, 5438 (1995).
[5] S. Y. Khlebnikov and I. I. Tkachev, Phys. Rev. Lett. **77**, 219 (1996); **79**, 1607 (1997).
[6] T. Prokopec and T. G. Roos, Phys. Rev. D **55**, 3768 (1997).
[7] J. Berges and J. Serreau, Phys. Rev. Lett. **91**, 111601 (2003); J. Berges, S. Borsanyi, and C. Wetterich, Phys. Rev. Lett. **93**, 142002 (2004).
[8] G. N. Felder and L. Kofman, Phys. Rev. D **63**, 103503 (2001).
[9] D. I. Podolsky, G. N. Felder, L. Kofman, and M. Peloso, Phys. Rev. D **73**, 023501 (2006).
[10] R. Micha and I. I. Tkachev, Phys. Rev. D **70**, 043538 (2004).
[11] A. D. Dolgov and A. D. Linde, Phys. Lett. **116B**, 329 (1982).
[12] L. F. Abbott, E. Farhi, and M. B. Wise, Phys. Lett. **117B**, 29 (1982).
[13] B. A. Bassett, S. Tsujikawa, and D. Wands, Rev. Mod. Phys. **78**, 537 (2006).
[14] J. F. Dufaux, G. N. Felder, L. Kofman, M. Peloso, and D. Podolsky, J. Cosmol. Astropart. Phys. 07 (2006) 006.
[15] N. Shuhmaher and R. Brandenberger, Phys. Rev. D **73**, 043519 (2006).
[16] B. R. Greene, T. Prokopec, and T. G. Roos, Phys. Rev. D **56**, 6484 (1997).
[17] P. B. Greene, L. Kofman, A. D. Linde, and A. A. Starobinsky, Phys. Rev. D **56**, 6175 (1997).
[18] D. I. Kaiser, Phys. Rev. D **56**, 706 (1997); **57**, 702 (1998).
[19] M. Abramowitz and I. Stegun, *Handbook of Mathematical Functions* (Dover, New York, 1970), p. 587.
[20] The Wolfram Functions Site, http://functions.wolfram.com/09.26.06.0002.01.